ACS APPLIED MATERIALS & INTERFACES

RESEARCH ARTICLE

www.acsami.org

Fluorinated Amphiphilic Polymers and Their Blends for Fouling-Release Applications: The Benefits of a Triblock Copolymer Surface

Harihara S. Sundaram,[†] Youngjin Cho,[†] Michael D. Dimitriou,[‡] John A. Finlay,[⊥] Gemma Cone,[⊥] Sam Williams,[¶] Dale Handlin,[¶] Joseph Gatto,[¶] Maureen E. Callow,[⊥] James A. Callow,[⊥] Edward J. Kramer,[‡,§] and Christopher K. Ober*[,†]

[†]Department of Materials Science and Engineering, Cornell University, Ithaca, New York 14853, United States

[‡]Department of Materials, University of California, Santa Barbara, California 93106, United States

[§]Department of Chemical Engineering, University of California, Santa Barbara, California 93106, United States

[⊥]School of Biosciences, The University of Birmingham, Birmingham, B15 2TT, United Kingdom

[¶]NanoSurfaces Inc., 8 Saint Mary's Street, Boston, Massachusetts 02215, United States

Supporting Information

ABSTRACT:

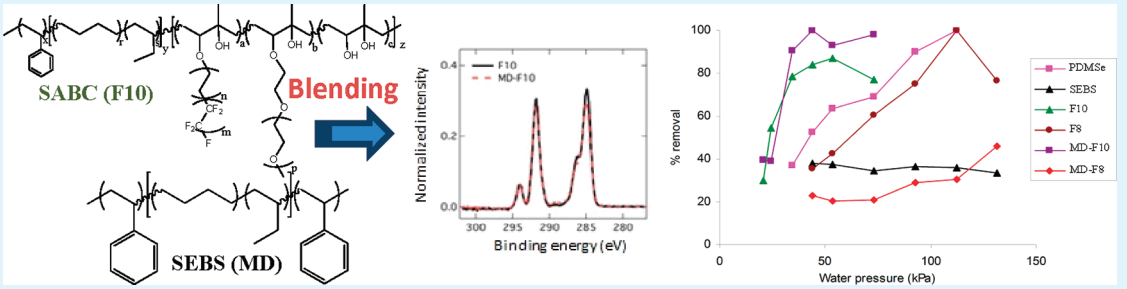

Surface active triblock copolymers (SABC) with mixed polyethylene glycol (PEG) and two different semifluorinated alcohol side chains, one longer than the other, were blended with a soft thermoplastic elastomer (TPE), polystyrene-*block*-poly(ethylene-*ran*-butylene)-*block*-polystyrene (SEBS). The surface composition of these blends was probed by X-ray photoelectron spectroscopy (XPS) and near edge X-ray absorption fine structure (NEXAFS) spectroscopy. The surface reconstruction of the coatings in water was monitored qualitatively by dynamic water contact angles in air as well as air bubble contact angle measurements in water. By blending the SABC with SEBS, we minimize the amount of the SABC used while achieving a surface that is not greatly different in composition from the pure SABC. The 15 wt % blends of the SABC with long fluoroalkyl side chains showed a composition close to that of the pure SABC while the SABC with shorter perfluoroakyl side chains did not. These differences in surface composition were reflected in the fouling-release performance of the blends for the algae, *Ulva* and *Navicula*.

KEYWORDS: surface active block copolymer, polymer blends, biofouling, amphiphilic block copolymer, surface segregation, low surface energy materials

INTRODUCTION

The control of surface composition and structure remains one of the key objectives in most coatings research. Block copolymers offer the ability to specifically tailor surface properties by designing one block to dominate the surface. This approach has been used to modify surface properties in a controlled way in uses ranging from surfaces for cell growth in tissue scaffolds,[1] stimuli-responsive surfaces,[2] self-cleaning surfaces for water purification membranes,[3] and in reversibly switching surfaces.[4] Modification of surface properties using block copolymers can be categorized into two approaches: first, a coating in its own right where one block interfaces with the substrate and the other dominates the surface, or second, blended with a host polymer where the surface is determined by the block copolymer and the coating mechanical properties are set by the host matrix. It has been shown that mixing a small amount of a low surface energy block copolymer into a homopolymer can produce a low energy surface by segregation of the block copolymer to the surface.[5] In most prior studies of surface control using polymer blends, the surface active block copolymer has been combined with a high

Received: April 29, 2011
Accepted: August 10, 2011
Published: August 10, 2011

molecular weight homopolymer (for example, polystyrene).[6−8] This combination enables the formation of a coating with the surface properties of the block copolymer with the mechanical properties of the host matrix.

However, there are circumstances where a rigid coating (such as that formed from polystyrene) with controlled surface energy or composition is insufficient. For example, for fouling-release behavior, a coating is needed with a much lower modulus than polystyrene can provide.[9] In our experience, surface active block copolymers blended with a thermoplastic elastomer (TPE) block copolymer matrix offer excellent properties.[10,11] Taking advantage of this fact, low surface energy blends have been previously prepared by mixing a semifluorinated monodendron surface active diblock copolymer with a styrene block containing thermoplastic elastomer (TPE) based on polystyrene-*block*-poly(ethylene-*co*-butadiene)-*block*-polystyrene (SEBS). In that work, it was shown, however, that for complete coverage of the surface with fluorinated segments, a blend with at least 35% of the surface active triblock copolymers (SABC) in a TPE was required.[8] However, the relatively large quantity of SABC needed to fully populate a coating surface has led to a focus on multilayer coatings as a means to achieve the necessary combination of surface and mechanical properties.[10] Recently, we have examined ABC triblock surface active block copolymers in which the C block contains surface active side groups and the A and B blocks were designed to be compatible with the SEBS used to establish the elastomeric properties needed in the coating.[12] As a result of the observed excellent surface coverage of this new triblock copolymer, we have reinvestigated the use of SABC/SEBS blends to produce effective fouling-release coatings.

Biofouling is an undesirable accumulation of microorganisms, plants, and/or animals on wetted structures.[13] The resulting drag on surfaces moving through water leads to a significant increase in the cost of maritime transportation.[14] Furthermore, slimes, dominated by diatoms (unicellular algae), on a ship's hull can also increase hydrodynamic drag, increasing fuel costs by up to 15%.[15] Adhesion of marine fouling organisms is facilitated by a range of materials including proteins, glycoproteins, and polysaccharides.[16,17] One strategy to control fouling is to design surfaces that reduce the tenacity of these adhesive bonds. *Ulva* (syn. *Enteromorpha*) is a common green macroalgae found throughout the world.[18] Diatoms (*Bacillariophyceae*, *Ochrophyta*) are a diverse and abundant group of unicellular algae that form adherent slimes on surfaces.[19,20] *Ulva* and diatoms, such as species of *Navicula*, are known to show opposite behavior in terms of adhesion, including to silicone fouling-release coatings.[21] Fouling-release coatings have specific physicochemical and bulk properties that affect the adhesion of fouling organisms, especially macrofoulers such as barnacles. Thus, the fouling organisms are "released" by hydrodynamic forces such as a ship moving through the water[22] or by gentle cleaning (grooming).[23] Biocides such as tributyltin (TBT) containing self-polishing coatings were the active components of the antifouling paints until its use was globally prohibited due to the toxicity of TBT in the environment.[24−26] The alternative heavy metal containing paints such as copper-containing antifouling paints also cause certain environmental concerns.[27] The major source of trace metals especially copper in harbors and heavily traveled waterways is antifouling bottom paints.[28]

To date, the most successful fouling-release commercial coatings have been constructed from cross-linked silicone elastomers.[9,29] Other strategies to achieve fouling release from model surfaces have been based on self-assembled monolayers,[30,31] zwitterionic,[32,33] and polyethylene glycol (PEG) based[34] polymer brushes and cross-linked block copolymers.[35−37] Microtopographic-patterned PDMS surfaces have also been found to show good antifouling for *Ulva*.[29,38] It is evident that control of surface composition and properties is critical in determining fouling behavior.

In the current study, we have used mixed amphiphilic triblock copolymers containing separately attached semifluorinated and PEG side chains for the surface-active block. On the basis of prior results, we anticipated that the surfaces of both the pure SABC and the blended polymer coatings will be dominated initially by the semifluorinated chains through surface segregation. Since the mixed side groups (semifluorinated and PEG chains) are uniformly distributed along the backbone of the C block, the surface properties will change upon immersion in water as the more hydrophilic PEG groups migrate to the surface after adsorption of water molecules. The presence of both of these groups on the surface forms the basis of an effective fouling-resistant and fouling-release coating.[10]

The work of this report focuses on the use of blending as an efficient method to create an effective coating and to improve its damage tolerance. The thermoplastic elastomer base polymer (SEBS) was used as a matrix and into it was blended the functional ABC triblock copolymer. We have found that triblock copolymer based surfaces combined with SEBS provide better coverage than comparable diblock copolymer surfaces. In this work, we have specifically investigated the surface composition, wetting, and foul-release properties of two SABCs having different chain lengths of semifluorinated chains in combination with polyethylene glycol chains. Two distinct semifluorinated side groups were studied, one containing a ten carbon long fluorinated segment combined with a ten carbon long hydrocarbon (F10H10, to make F10 SABC) while the other consisted of an eight carbon long fluorinated segment combined with a six carbon long hydrocarbon unit (F8H6, to make F8 SABC). Both the F8 SABC and F10 SABC incorporated a 550 g/mol PEG unit as the polar side chain of the C block. Blends of these SABCs with SEBS were used as the surface coating material, each containing significantly less SABC than that used for our earlier studies of diblock copolymer based fouling-release materials.[10,12,39] Antifouling or the antisettlement and fouling-release performance of the pure SABCs and their blends were compared. To identify an appropriate composition for each side group, preliminary fouling-release tests with a series of mixed amphiphilic SABC triblock copolymers were performed with a targeted top layer thickness of ∼1 μm. The polymers included mixed amphiphilic polymers from the F10/PEG series and from the F8/PEG series. From this experiment, two polymers (one each from the F10/PEG and F8/PEG combinations) were chosen and used for further studies. All four polymeric coatings (two pure SABCs and two blends) were thoroughly characterized by X-ray photoelectron spectroscopy (XPS) and near edge X-ray absorption fine structure (NEXAFS) spectroscopy. The surface amphiphilicity was also investigated using dynamic water contact angle and air bubble contact angle experiments. The antifouling and fouling-release performance of these coatings was also tested against the common fouling algae, *Ulva* and *Navicula*.

EXPERIMENTAL SECTION

Materials. Polystyrene$_{8K}$-*block*-poly(ethylene-*ran*-butylene)$_{25K}$-*block*-polyisoprene$_{10k}$ (PS_{8k}-*b*-$P(E/B)_{25k}$-*b*-PI_{10k}) triblock precursor

copolymer was produced by Kraton Polymers using anionic polymerization with subsequent catalytic hydrogenation. 1-Iodoperfluorodecane ($I(CF_2)_{10}F$, 98%) and 1-iodoperfluorooctane ($I(CF_2)_8F$, 98%) were purchased from Synquest Laboratories and used as received. 9-Decen-1-ol ($H_2C{=}CH(CH_2)_8OH$, 97%), 5-hexen-1-ol ($H_2C{=}CH(CH_2)_4OH$, 97%), 2,2′-azobis(2-methylpropionitrile) (AIBN, $NCC(CH_3)_2NNC(CH_3)_2CN$, 98%), and tributyltin hydride ($(n\text{-}Bu)_3SnH$, 97%) were purchased from Sigma-Aldrich and used as received in conjunction with the iodoperfluorocarbon to synthesize 1,1,1,2,2,3,3,4,4,5,5,6,6,7,7,8,8,9,9,10,10-henicosafluoroicosane (10-perfluorodecyl-1-decanol; F10H10OH) and 1,1,1,2,2,3,3,4,4,5,5,6,6,7,7,8,8-heptadecafluoro-tetradecane (8-perfluorooctyl-1-hexanol; F8H6OH) using procedures reported earlier.[39,40] 3-*meta*-Chloroperoxybenzoic acid (*m*CPBA, ClC_6H_4COOOH, 77%), boron trifluoride diethyl etherate ($BF_3{\bullet}Et_2O$, 99.9%), and poly(ethylene glycol) methyl ether (PEG550, $CH_3(OCH_2CH_2)_xOH$, average $M_n \approx 550$ g/mol, $x \approx 12$) were purchased from Sigma Aldrich and used as received in the modification of the PS-*b*-P(E/B)-*b*-PI triblock precursor polymers. Toluene, methanol, 6.25 N sodium hydroxide, 96% sulfuric acid, 30 wt % hydrogen peroxide in water, 95% ethanol, and all other reagents were used as received. 3-(Aminopropyl)-trimethoxysilane (APTMS, 99%) was purchased from Gelest and used as received. Polystyrene-*block*-poly(ethylene-*ran*-butylene)-*block*-polystyrene (SEBS) triblock thermoplastic elastomers (Kraton MD6945) and SEBS grafted with maleic anhydride (MA-SEBS, Kraton FG1901X) were generously provided by Kraton Polymers.

Characterization. ^{1}H NMR spectra were recorded using a Varian Gemini spectrometer with deuterated chloroform at 400 MHz. The IR spectra of the polymers cast as films from THF solution on sodium chloride plates were collected using a Mattson 2020 Galaxy Series FTIR spectrometer. Gel permeation chromatography of a THF solution of polymers (1 mg/mL) was carried out using four Waters Styragel HT columns operating at 40 °C in conjunction with Waters 490 ultraviolet (λ = 254 nm) and Waters 410 refractive index detectors. The molecular weight range of the columns was from 500 to 107 g/mol. THF was used as the eluent at a flow rate of 1 mL/min, and toluene was used as a marker for flow calibration.

Polymer Synthesis and Characterization. Surface active block copolymers were synthesized through a two step modification of the Kraton PS-*b*-P(E/B)-*b*-PI precursor polymers reported earlier.[12,39] The polyisoprene block of the PS-*b*-P(E/B)-*b*-PI polymer was epoxidized and ring opened with mixtures of F10H10OH and PEG550 with a molar feed ratio of 4:6 for F10. For F8, the epoxidized polymer was ring opened with mixtures of F8H6OH and PEG550 with a molar feed ratio of 8:2. The percent attachment of the side chains were calculated from ^{1}H NMR and elemental analysis as reported earlier.[39]

^{1}H NMR for epoxidized PS-*b*-P(E/B)-*b*-PI (400 MHz, $CDCl_3$, δ): 6.57, 7.07, (5H, styrene), 2.66 (br s, 1H, epoxidized isoprene, $-CH_2\boldsymbol{H}COC(CH_3)CH_2-$); 0.80, 1.07, 1.22, 1.45, 1.57 (backbone). IR (dry film) υ_{max} (cm $^{-1}$): 2925, 2850 (C−H stretching); 1470 (C−H bending); 1070 (C−O stretching); 880 (C−O−C stretching); 700 (C−H bending, aromatic).

^{1}H NMR for PS-*b*-P(E/B)-*b*-PI functionalized with F10H10OH/PEG550 side chains (400 MHz, $CDCl_3$, δ): 6.6, 7.1, (5H, styrene), 3.6 (br s, 4H $-OC\boldsymbol{H}_2C\boldsymbol{H}_2O-$); 0.8, 1.1, 1.24, 1.8 (polymer backbone). IR (dry film) υ_{max} (cm $^{-1}$): IR (dry film) υ_{max} (cm $^{-1}$): 3450 (O−H stretching); 2935, 2865 (C−H stretching); 1455, 1375 (C−H bending); 1120 (C−O stretching); 700 (C−H bending, aromatic); 1220 (C−F stretching).

Surface Preparation and Characterization. The glass slides for bioassays were made as reported earlier.[12,39,46] In summary, glass slides were cleaned by immersion in a mixture of concentrated H_2SO_4 and 30 wt % H_2O_2 solution (in a 7:3 v/v), rinsed, and then dried. The surface was then kept in 4% w/v solution of 3-(aminopropyl)-trimethoxysilane (APTMS) in ethanol. The glass slides were then cured at 110 °C under reduced pressure for a minimum of 30 min. This amine containing silane served as an adhesion promoter for the initial SEBS layer which was spin coated as a mixture of 5% MA-SEBS and 2% MD6945 in cyclohexane and spin coated. This was followed by successive spin coating of a 12% w/v SEBS (MD6945) solution in cyclohexane three times. Finally, a relatively thin layer of SABC or the blend (SABC/SEBS) was applied by spray coating from a 0.12% w/v solution in cyclohexane. The glass slides were annealed overnight at 60 °C for 24 h and 120 °C for 24 h under reduced pressure. Sufficient material was sprayed to produce an approximately 1 μm thick coating for the SABC only surface and 20 μm thick coating for the blends. The surfaces were annealed in a vacuum oven at 60 °C for 24 h and then at 120 °C for 24 h in a high vacuum oven. XPS measurements were performed using a Kratos Axis Ultra Spectrometer (Kratos Analytical, Manchester, UK) with a monochromatic Al Kα X-ray source (1486.6 eV) operating at 225 W under a vacuum of 1.0×10^{-8} Torr. Charge compensation was carried out by injection of low-energy electrons into the magnetic lens of the electron spectrometer. The pass energy of the analyzer was set at 20 eV for high-resolution spectra with an energy resolution of 0.05 eV. The spectra were analyzed using CasaXPS v.2.3.14 software. The C−C peak at 285 eV was used as the reference for binding energy calibration.

NEXAFS experiments were carried out on the U7A NIST/Dow materials characterization end-station at the National Synchrotron Light Source at Brookhaven National Laboratory (BNL). The general underlying principles of NEXAFS and a description of the beamline at BNL have been previously reported.[41,42] The X-ray beam was elliptically polarized (polarization factor = 0.85), with the electric field vector dominantly in the plane of the storage ring. The photon flux was approximately 1×10^{11} photons per second at a typical storage ring current of 750 mA. A spherical grating monochromator was used to obtain monochromatic soft X-rays at an energy resolution of 0.2 eV. The C 1s NEXAFS spectra were acquired for incident photon energy in the range of 270−320 eV. The angle of incidence of the X-ray beam, θ measured from the sample surface, was varied so as to check for molecular orientation on the surface layer and to permit a rough depth profiling.[43−45] The partial-electron-yield (PEY) signal was collected using a channeltron electron multiplier with an adjustable entrance grid bias (EGB). Data were reported for a grid bias of −150 V. The channeltron PEY detector was positioned at an angle of 35° above the equatorial plane of the sample chamber and at an angle of 36° in that plane relative to the incoming X-ray beam.[44] The PEY C 1s spectra were normalized by subtracting a linear pre-edge baseline and setting the edge jump to unity at 320 eV. The photon energy was calibrated by adjusting the peak position of the lowest π^* phenyl resonance from polystyrene to 285.5 eV.

Water contact angles were measured using a contact angle goniometer (AST Products, Inc. model VCA Optima XE) at room temperature. Dynamic water contact angle measurements were performed through the addition and retraction of a small drop of water (ca. 2 μL) on the surface. The advancing and receding contact angle behavior was digitally recorded, and image analysis software was used to measure the angles. The contact angle of an air bubble under an inverted polymer surface immersed in water was determined using the captive bubble method. An air bubble, which was detached from the tip of a 22 gauge stainless steel syringe needle (0.7 mm o.d. and 0.4 mm i.d.), was placed in contact with the water immersed surface and used to measure the contact angle. The angles reported are measured between the surface and the air bubble on the water side. Thus, a low captive-bubble contact angle indicates a hydrophilic surface, while a higher angle indicates a more hydrophobic surface.[46] The surface roughness of the spray coated surfaces were measured using a stylus based P10 profilometer. The stylus force used was 3.0 mg, and the scanning was performed for a length of 500 μm.

Preparation of Coated Surfaces for Algal Bioassays. Glass slides coated with SABCs based on the PS-*b*-P(E/B)-*b*-PI precursor subsequently were prepared in an analogous fashion using Kraton MD6945 SEBS which has similar elastic modulus to that of PDMS.[12,39,47] For all biofouling assays, glass microscope slides coated with a poly(dimethylsiloxane) elastomer (PDMSe), Silastic T2 (DowCorning) supplied by Professor A. B. Brennan, University of Florida, and prepared as described by Schumacher et al.[47] were included as standards, and slides coated with MD6945 SEBS were included as controls. PDMSe was used as a standard due to its excellent release properties against macrofouling organisms such as *Ulva* sporelings,[48] while MD6945 base layers were used to highlight the differences in performance between the base layer alone and with the SABC multilayer coatings.

Settlement of Zoospores and Strength of Attachment of Sporelings (Young Plants) of *Ulva*. Nine replicates of each test sample were equilibrated in a 30 L tank of recirculating deionized water at ~20 °C for 48 h before being transferred to artificial seawater (ASW) 1 h prior to the start of the assays. Zoospores were obtained from mature *Ulva* plants by the standard method.[48] In brief, 10 mL of a suspension of zoospores (1×10^6 spores/mL) was added to test surfaces, each in an individual compartment of quadriperm dishes (Greiner One). The dishes were incubated in the dark at ~20 °C for 45 min, and then, each test slide was washed in ASW to remove zoospores that had not attached, i.e., were still motile. Three replicate slides of each type were fixed using 2.5% glutaraldehyde in seawater and were used to quantify the density of zoospores attached to the surfaces using an image analysis system attached to a fluorescence microscope as reported earlier.[49]

The remaining six replicates of each coating were used to culture sporelings (young plants).[9] After washing away unattached spores, the samples were transferred to dishes containing nutrient enriched seawater and grown for 7 days under an 18h:6 h light:/dark regime at 18 °C, with the culture medium being refreshed every 48 h. Biomass was estimated by direct measurement of fluorescence, from chlorophyll contained within the chloroplasts of the sporelings, using a Tecan plate reader (GENios Plus).[49] Fluorescence was recorded in terms of relative fluorescence units (RFU). The strength of attachment of the sporelings was determined by exposing the central area of biomass to an impact pressure delivered by a calibrated water jet apparatus.[17] The range of impact pressures used was chosen to provide maximum information about the strength of attachment of the sporelings. RFU readings were taken within the part which was exposed to a water jet. The percentage removal was calculated from readings taken before and after water jetting.

Attachment and Adhesion Strength of *Navicula*. *Navicula* cells were cultured in F/2 medium contained in 250 mL conical flasks. After 3 days, the cells were in log phase growth. Cells were washed 3 times in fresh medium before harvesting and diluting to give a suspension with a chlorophyll content of approximately 0.25 μg mL^{-1}. Ten milliliters of culture were added to individual compartments of dishes, which were left on the laboratory bench at ~20 °C for 2 h. The slides were exposed to a submerged wash in seawater to remove cells which had not attached (the immersion process avoided passing the samples through the air−water interface, which can lead to cell clumping on hydrophobic surfaces). Samples were fixed in 2.5% glutaraldehyde and air-dried, and the density of cells attached to the surface was counted as for spores of *Ulva*. Washed slides with attached cells were exposed to a shear stress of 52 Pa in a water channel.[50] Samples were fixed, and the number of cells remaining attached was counted using the image analysis system described above.

RESULTS AND DISCUSSION

The structures of the functional SABC polymers synthesized are represented in Scheme 1. The percentage attachment of PEG was calculated from ^{1}H NMR, and the percentage attachment of semifluorinated alcohol was calculated from elemental analysis. (More detail is provided in Supporting Information.) The compositions of these polymers are shown in Table 1. While the molar percentage attachment of the fluoroalkyl side groups for both the F10 and the F8 SABCs is nearly the same, there is significantly higher attachment of the PEG groups for the F10 than for the F8. These SABC block copolymers were blended with SEBS to form the 15 wt % blends MD-F10 and MD-F8 of the respective SABCs in SEBS.

Scheme 1. Structure of Mixed Amphiphilic Surface-Active Block Copolymer Modified with a Mixture of Semifluorinated and PEG Chains

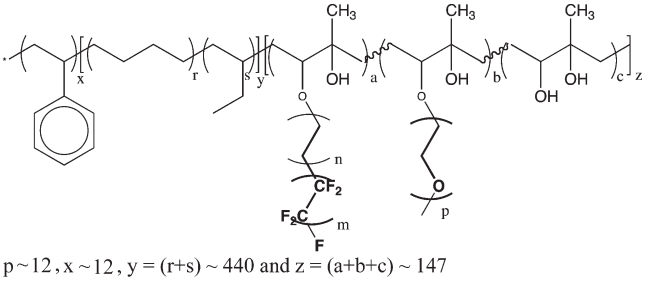

p ~ 12 , x ~ 12 , y = (r+s) ~ 440 and z = (a+b+c) ~ 147
m = 4 and n = 3 for F8; m = 5 and n = 5 for F10

Table 1. Composition of the Functional Polymer Coatings Used

SABC			polymer blends	
	mol % attachment			
polymer	PEG	semifluorinated chains	blend	composition
F10	24.5	22.6	MD-F10	15 wt % of F10
F8	8.0	22.0	MD-F8	15 wt % of F8

In the current study, the molecular weight of the SABC was designed to be morphologically consistent with the SEBS. Their polystyrene blocks are approximately the same (PS (M_n) ~ 8000 g/mol), and the poly(ethylene-*ran*-butylene) block of the SABC is one-half that of the SEBS. This should allow better mixing of the two polymers when cast from a common solvent. Blending the SEBS, a thermoplastic elastomer, with the SABC should improve the mechanical properties of the coatings and its adhesion to underlying SEBS layers. Blending also allows the bulk coating to serve as the reservoir of the low surface energy SABC block copolymer which could segregate to the surface if the surface is eroded or abraded.

Polymer Surface Coating and Characterization. The schematic representation of the multilayer coating used for fouling release studies is given in Figure 1.

Both the SABC and SABC/SEBS blend coatings were prepared on top of separate SEBS thermoplastic elastomer base layers by spray coating. The target thickness for the SABC was ~1 μm, and the target for the SABC/SEBS blends was ~20 μm. The quantity of polymer used for making these coatings was significantly less than the amount of SABC used for earlier biofouling studies by our group.[12,39] The surface properties of

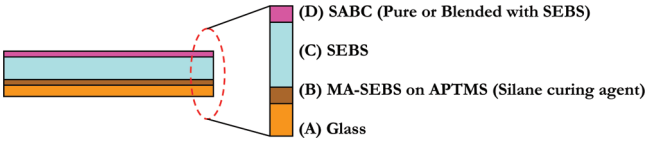

Figure 1. Schematic representation of the multilayer coating used for the fouling release studies.

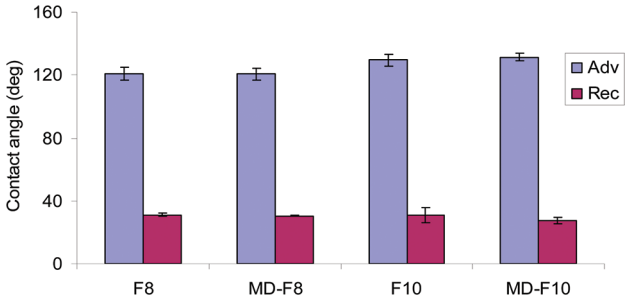

Figure 2. Advancing and receding water drop contact angles of the mixed amphiphilic polymers and their blends with MD6945 SEBS spray coated on top of SEBS-coated glass slides.

the SABC/SEBS blends were compared to surfaces produced directly from the SABC alone on the SEBS.

Contact Angle Studies. The behaviors of the unmodified SABC and the epoxidized SABC have been reported earlier.[12] The unmodified SABC has advancing contact angles in the range of 90° with a large hysteresis while the epoxidized and hydrolyzed SABC has advancing contact angle values in the range of 50°. The contact angle of a water drop on the surfaces of SABCs and their blends are shown in Figure 2. Here, the advancing contact angles are slightly higher for both the F10 SABC and its blends relative to the F8 SABC and its blend. The very high advancing contact angles of MD-F8 and MD-F10 suggest that the semifluorinated side groups of the SABCs segregate to the surface of the blend[6,39] even though the SABC is only 15 wt % of the blend. The receding contact angle is approximately constant at 30° for all polymers. The large contact angle hysteresis can be attributed to the surface rearrangement as well as to surface roughness. The surface roughness of all the spray coated films is on the order of 4–5 μms rms using a profilometer, but this roughness is over a large lateral length scale as the AFM scans on a 1 × 1 μm length scale show a surface both in air and under water that is much smoother, with a roughness of at most a few nms, as shown in the Supporting Information.

Air Bubble Contact Angle. Air bubble contact angle measurements were performed to study the rearrangement of the amphiphilic side chains on the surface of the coatings. All of the polymers showed an immediate drop in contact angle within hours of immersion in water. The advancing contact angle continued to decrease slowly over a period of days and reached a value of ~25° or less over 2 weeks. This result suggests that the PEG side chains of the amphiphilic polymers migrate to the surface when immersed in water. The behavior of all four samples is surprisingly similar despite the significant difference in PEG content. This indicates that even the blended samples with the lowest PEG content contain enough PEG to change the hydrated surface properties. The same trend has been noted with amphiphilic side chain SABCs.[10,11]

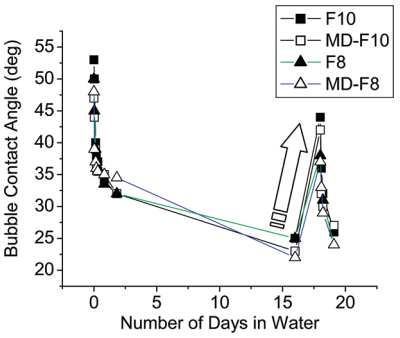

Figure 3. Underwater air bubble contact angle measured on the different SABC polymers spray coated on glass slides. The arrow mark indicates an increase in the bubble contact angle after reannealing the polymer coating at 120 °C for 12 h.

These coatings were removed from water and then reannealed at 120 °C for 12 h to study the recovery behavior of the surface. All the polymers showed a significantly higher bubble contact angle after reannealing, followed by a decline in this value over time. Annealing apparently led to only partial recovery of the original surface because the contact angles did not reach the levels measured from the original surfaces. While the surfaces of the F8 SABC side chain modified polymer and its blend also reconstructed to produce higher contact angle values, the F10 SABC polymers and its blends had larger contact angles after the 120 °C, 12 h anneal. This result demonstrates that F10 groups provide a stronger driving force to populate the surface in air despite the fact that the F10 SABC has the same number of fluorinated side groups and a more than 3-fold higher attachment of hydrophilic PEG groups compared to the F8 SABC.

The NEXAFS data for the F10 SABC polymer and its blend (MD-F10) spray coated on top of an SEBS base layer are shown in Figure 4. The shoulder peak near 288 eV can be attributed to the C 1s → σ^*C−H signal. The characteristic signals near 293 and 295.8 eV are indicative of both the C 1s → σ^*C−F and C 1s → σ^*C−C resonances from the $-CF_2-$ helix, demonstrating the presence of the fluoroalkyl groups on the surfaces. The fact that these peaks increase in height at angles greater than 90° indicates that the $-CF_2-$ helices are within 1 to 2 nm of the surface (at these angles, the effective escape depth of the Auger electrons decreases dramatically with θ), but a detailed analysis of the data between θ = 30 and 90° shows that there is little, if any, orientation of the helices relative to the surface normal.[41,42] On comparing the intensities of the peaks between the pure F10 polymer and its blend, there is not much difference in the intensities of C−F peaks. There is no peak around 285.5 eV characteristic for C 1s → π^*C═C derived from the polystyrene block. This also shows that the SABCs are very effective in populating the surface and there is no significant presence of polystyrene on the surface even for the blended samples.

The NEXAFS data for the F8 polymer and its blend (MD-F8) spray coated on top of the SEBS base layer are shown in the Figure 5. The characteristic 293 and 295.8 eV peaks due to the C 1s → σ^*C−F and C 1s → σ^*C−C resonances from the $-CF_2-$ helix are present in both the F8 SABC film and the 15 wt % blend with SEBS, but the peaks are significantly lower in the blend. Moreover, a very small C 1s → π^*C═C peak due to the polystyrene block was observed for the F8 SABC blended polymer which was absent for the F8 pure SABC coated surface.

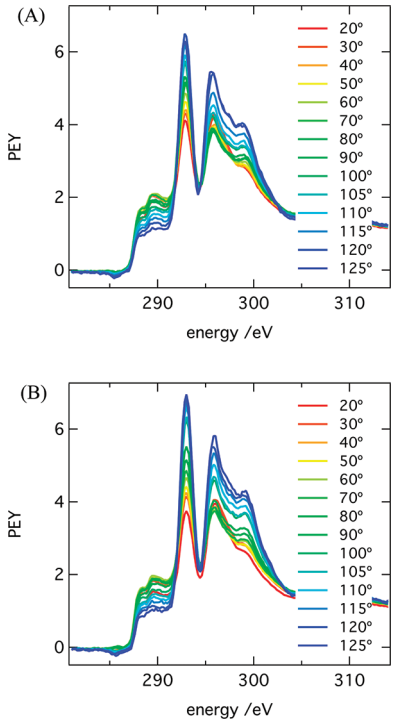

Figure 4. NEXAFS spectra of spray coated polymer films of F10 SABC (A) and MD-F10 (B) on top of a SEBS layer. The different spectra were taken with different values of θ, the angle between the surface normal and the soft X-ray beam.

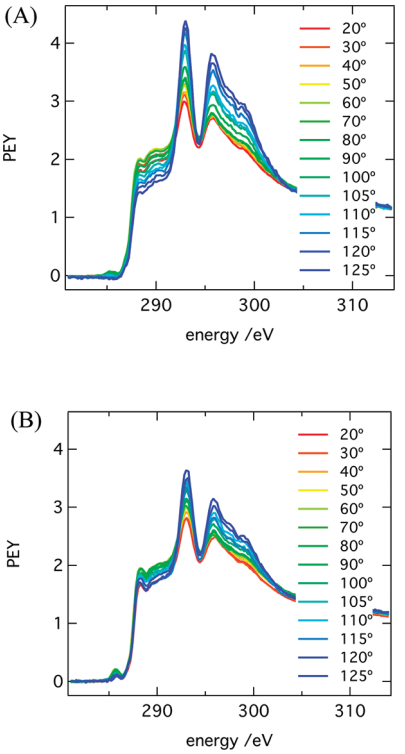

Figure 5. NEXAFS spectra of spray coated polymer films of F8 (A) and MD-F8 (B) on top of a SEBS layer. The different spectra were taken at different values of θ, the angle between the surface normal and the soft X-ray beam.

The F8 SABC, while present on the surface of the blend of this composition, is not as effective at covering the surface as the F10 SABC at the same wt % addition. These differences cannot be attributed to the attachment of the fluoroalkyl group (nearly identical for the two SABCs) or to the higher attachment of hydrophilic and high surface energy PEG groups on the F10 SABC copolymer but rather must be caused by the different surface activity of the F10 and F8 groups.

The XPS spectra of the F8 polymer and its 15 wt % blend with SEBS are shown in the Figure 6. These were taken at two different electron emission angles (0° and 75°) relative to the surface normal. The high resolution spectra are normalized so that the total area under the carbon peaks is equal to unity. There are characteristic peaks for $-CF_3$ (294 eV) and $-CF_2-$ (292 eV) groups along with the C−O−C (286 eV) and C−C (285 eV) carbons. The figure shows that the intensities of the $-CF_3$ and $-CF_2-$ carbon peaks of the blended polymers are decreased relative to those of the pure F8, indicating a lower concentration of fluorine in the surface region for the blend. In addition, there is a significantly lower C−O−C peak for the blend, indicating that the amphiphilic block itself is less abundant at the surface.

The XPS data for the F10 copolymer and its blend with SEBS are shown in the Figure 7. Characteristic peaks for the $-CF_3$, $-CF_2-$, and C−O−C functional groups are present in the spectra. When these spectra are compared with those of F8 polymers, the intensities of the peaks for the carbons $-CF_3$ and $-CF_2-$ are higher in the F10 polymers. On comparing the intensities of the peaks for $-CF_3$ and $-CF_2-$ carbons for F10 and MD-F10, it is evident that both the coatings have their surface covered with roughly the same high concentration of the semifluorinated chains. This highlights the better efficiency of the F10 groups in both migrating to and covering the surface compared to the F8 segments especially when coupled to the triblock copolymer architecture. The PEG groups are also present just under both surfaces which is evident from the appearance of a peak at 286 eV for C−O−C. When the surface is probed deeper with an emission angle of 0°, this peak is strong. With an emission angle of 75°, where the experiment is more surface sensitive, this peak is very weak. The surface characterization illustrates the fact that the semifluorinated chains are efficient in segregating to the surface, as reported earlier for other semifluorinated side chain polymers.[39,51] A recent report by Mielczarski et al. described the surface segregation of semifluorinated chains in a matrix of silicone polymers.[52] The surface segregation was greater for the long semifluorinated side chains (F8 in our notation) than a shorter semifluorinated side chain (F6 in our notation).[52] We have also observed the same trend of migration of the semifluorinated chains among the F10 and F8 polymers. To summarize, a longer fluorinated segment leads to more surface segregation and greater surface coverage even though the longer fluorinated side chain is attached to a block that also has a 3-fold larger attachment of high surface energy PEG groups.

Antifouling and Fouling-Release Studies. The spore settlement data showed that the density of spores of *Ulva* attached to the SEBS control surface was high compared to that on all the functional polymer coated surfaces (Figure 8). This showed that all the functional polymers coated on the SEBS layers substantially altered the properties of the SEBS surface. It is again evident that the functional chains have migrated to the surface of the blended polymers and by affecting the surface properties alter the

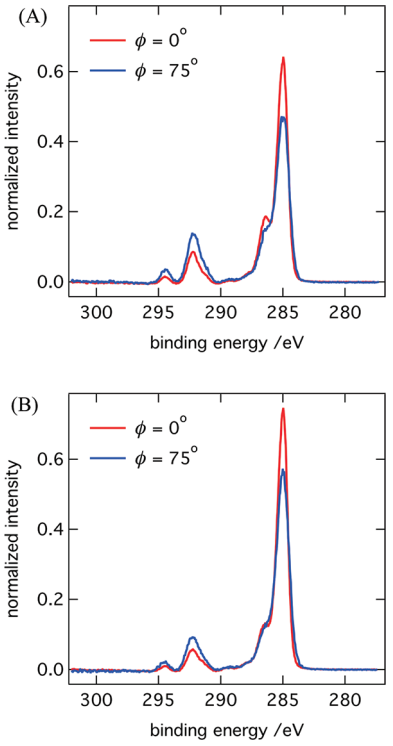

Figure 6. XPS spectra of spray coated polymer films of F8 (A) and MD-F8 (B) on top of SEBS layer taken at two different electron emission angles (0° and 75°) relative to the surface normal. The high resolution spectra are normalized so that the total area under the carbon peaks is equal to unity.

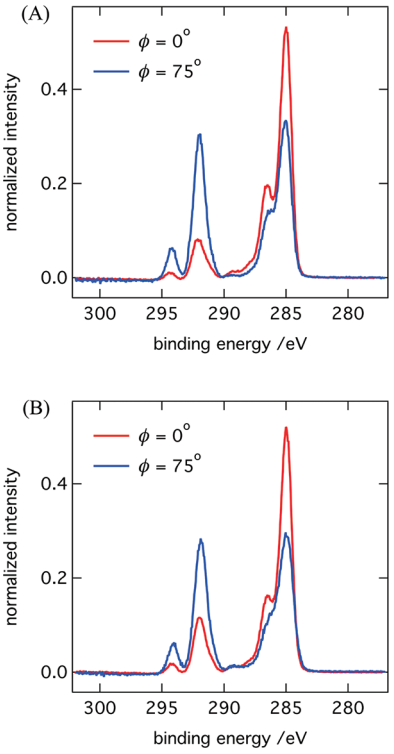

Figure 7. XPS spectra of spray coated polymers films of F10 (A) and MD-F10 (B) on top of SEBS layer taken at two different electron emission angles (0° and 75°) relative to the surface normal. The high-resolution spectra are normalized so that the total area under the carbon peaks is equal to unity.

settlement density of spores. On the basis of the data in Figure 3, a significant amount of surface reconstruction would have taken place at the time the assay was started (48 h immersion), although the captive bubble data suggest that this would not have been complete for several more days of immersion.

Sporelings (young plants) formed a green lawn on the surface of all coatings after 7 days of growth. The F10 based SABC coatings released about 80% of the biomass of sporelings on the film surface at a water jet pressure of ~25 kPa (Figure 9). For the same extent of release, the PDMSe surface required ~80 kPa water jet pressure. The release data for sporelings showed that both the F10 polymer and its blend were superior to the standard PDMSe surface. The F8 SABC also showed reasonable fouling release but had lower performance compared to the standard PDMSe. The F8 blend performed poorly with release characteristics similar to that of the SEBS base polymer. This result is surprising given the nearly identical contact angle results for the F8 sample and its blend.

The density of cells of *Navicula* remaining on the test surfaces after washing and exposure to a wall shear stress of 52 Pa is shown in Figure 10. The data show that only F10 and its blend were effective in reducing the density of cells below that on the PDMSe. The F8 SABC and its blend supported a similar or higher density of cells as the SEBS control. The difference in cell density between the F8 and F10 samples is surprising since adhesion is typically correlated with wettability of the surfaces, exemplified by the low number of cells on the hydrophilic glass compared to the relatively high number on the hydrophobic PDMSe.[53] As noted above, the contact angle data in Figure 3 suggest that all samples should have similar biological

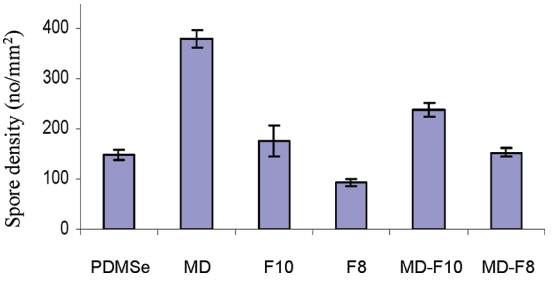

Figure 8. Settlement densities of spores of *Ulva* on PDMSe (a reference sample composed of Silastic T2), MD6945 SEBS control, and MD6945 SEBS coated with F10 and F8 SABCs and with the 15 wt % blends of the F10 and F8 SABCs with MD6945 SEBS.

performance. However, the combined fouling-release performance of the F10 SABC and MD-F10 against both *Ulva* and *Navicula* indicates that these coatings would be suited for fouling-release applications for a wider range of organisms.

The fouling-release properties of the two pure SABCs against *Ulva* sporelings are slightly different. Better performance of the SABC with longer semifluorinated chains (F10) compared to that with shorter semifluorinated chains (F8) is consistent with the surface characterization results. The *Ulva* sporeling removal results are revealing. While the release profile for the SABC with shorter semifluorinated chain (F8) was only slightly lower than that of the PDMSe standard, the profile for its blend showed much lower release behavior. The SABC with longer

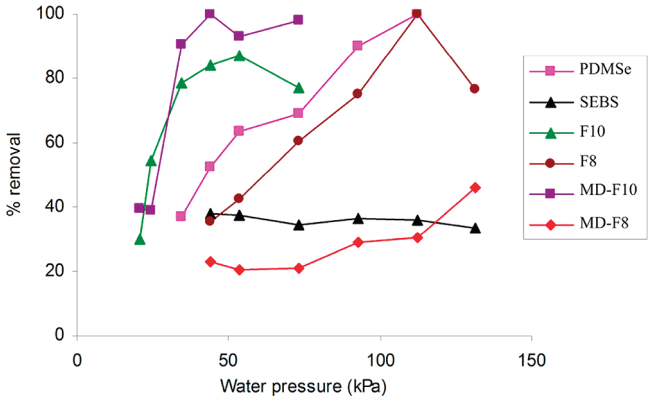

Figure 9. Percent removal of 7 day old sporelings of *Ulva* from amphiphilic coatings plotted as a function of surface water pressure (kPa). Coatings were exposed to a range of different surface pressures from the water jet. PDMSe is a reference sample composed of Silastic T2 and SEBS is a MD6945 SEBS control.

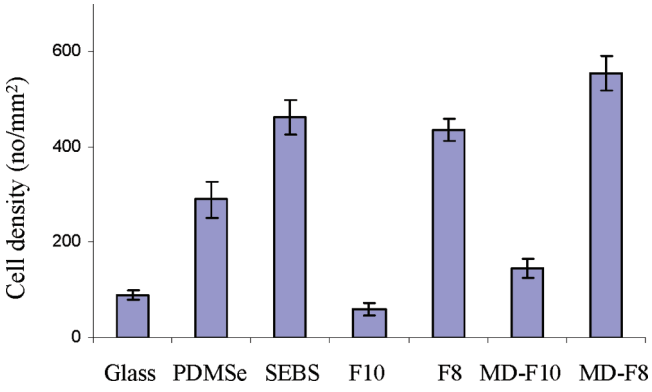

Figure 10. Final density of attached diatoms on amphiphilic coatings after gentle washing and exposure to a shear stress of 52 Pa. Bars show 95% confidence limits.

semifluorinated chains (F10) had an excellent release performance, in fact, better than that of the PDMSe standard. The blend of this polymer (MD-F10) also showed very good release performance compared to the PDMSe standard. Furthermore, this blended coating showed excellent performance compared to that of the pure SABC itself. This may be due to the fact that during processing the low surface energy functional groups segregate more to the surface compared to the pure SABC polymer. The better fouling-release performance may also be explained by the fact that this blended polymer coating has a soft TPE (SEBS) component throughout the coating which enhances its fouling-release performance in combination with reversible surface changes.

CONCLUSION

Amphiphilic polymers with mixtures of semifluorinated and polyethylene glycol side chains were synthesized and their surface properties were studied. The pure SABCs were blended with a soft thermoplastic elastomer (SEBS) and their surface properties were compared. There were two types of SABCs selected for the blending experiment that differed by the length of the fluorinated segment and the amount of PEG relative to the fluorinated component. Surface characterization using XPS and NEXAFS showed that the low surface energy groups populated the surface. The efficiency of the longer semifluorinated F10H10 chains to segregate to the surface is higher than that of the shorter semifluorinated F8H6 chains. The better surface segregating properties of the F10 polymers resulted in better fouling-release performance compared to the F8 chains containing functional polymer coatings. In the case of the F10 polymers, the fouling-release performance may also be enhanced by the presence of a higher amount of PEG chains which have a significant role to play when the coatings are exposed to water. This work illustrates the fact that blending a small quantity of a surface active functional polymer can be effective for fouling-release applications if a suitable combination of matrix and surface active polymers are chosen.

ASSOCIATED CONTENT

Supporting Information. Information concerning the calculation of SABC composition, AFM data of the surfaces in the dry and wet states, and data concerning the surface roughness of the samples. This material is available free of charge via the Internet at http://pubs.acs.org.

AUTHOR INFORMATION

Corresponding Author

*E-mail: cko3@cornell.edu. Tel: 607-255-8417. Fax: 607-255-2365.

ACKNOWLEDGMENT

This work was primarily supported by NanoSurfaces Inc (SHS). Partial support was provided by the U.S. Department of Defense's Strategic Environmental Research and Development Program (SERDP), grant WP #1454, with additional support from the Office of Naval Research (ONR) through awards #N00014-08-1-0010 (J.A.C. and M.E.C.) and N00014-02-1-0170 (C.K.O. and E.J.K.). Partial support from the Cornell KAUST Center is also acknowledged. E.J.K. and M.D.D. acknowledge partial support from the NSF Polymers Program (DMR-0704539) as well as the use of central facilities funded by the NSF-MRSEC program (UCSB MRL, DMR-0520415).

REFERENCES

(1) Yang, X.-Z.; Sun, T.-M.; Dou, S.; Wu, J.; Wang, Y.-C.; Wang, J. *Biomacromolecules* **2009**, *10*, 2213–2220.
(2) Bousquet, A.; Ibarboure, E.; Papon, E.; Labrugere, C.; Rodriguez-Hernandez, J. *J. Polym. Sci., Polym. Chem.* **2010**, *48*, 1952–1961.
(3) Wang, J.; Xu, Y.; Zhu, L.; Li, J.; Zhu, B. *Polymer* **2008**, *49*, 3256–3264.
(4) Reihs, K.; Voetz, M. *Langmuir* **2005**, *21*, 10573–10573.
(5) Shull, K. R.; Kramer, E. J.; Hadziioannou, G.; Tang, W. *Macromolecules* **1990**, *23*, 4780–4787.
(6) Iyengar, D. R.; Perutz, S. M.; Dai, C. A.; Ober, C. K.; Kramer, E. J. *Macromolecules* **1996**, *29*, 1229–1234.
(7) Hwang, S. S.; Ober, C. K.; Perutz, S.; Iyengar, D. R.; Scheneggenburger, L. A.; Kramer, E. J. *Polymer* **1995**, *36*, 1321–1325.
(8) Hexemer, A.; Sivaniah, E.; Kramer, E. J.; Xiang, M.; Li, X.; Fischer, D. A.; Ober, C. K. *J. Polym. Sci., Part B: Polym. Phys.* **2004**, *42*, 411–420.
(9) Chaudhury, M. K.; Finlay, J. A.; Chung, J. Y.; Callow, M. E.; Callow, J. E. *Biofouling* **2005**, *21*, 41–48.

(10) Krishnan, S.; Ayothi, R.; Hexemer, A.; Finlay, J. A.; Sohn, K. E.; Perry, R.; Ober, C. K.; Kramer, E. J.; Callow, M. E.; Callow, J. A.; Fischer, D. A. *Langmuir* **2006**, *22*, 5075–5086.
(11) (a) Martinelli, E.; Fantoni, C.; Galli, G.; Gallot, B.; Glisenti, A. *Mol. Cryst. Liq. Cryst.* **2009**, *500*, 51–62. (b) Martinelli, E.; Menghetti, S.; Galli, G.; Glisenti, A.; Krishnan, S.; Paik, M. Y.; Ober, C. K.; Smilgies, D. M.; Fischer, D. A. *J. Polym. Sci., Part A: Polym. Chem.* **2009**, *47*, 267–284.
(12) Weinman, C. J.; Finlay, J. A; Park, D.; Paik, M. Y.; Krishnan, S.; Sundaram, H. S.; Dimitriou, M.; Sohn, K. E.; Callow, M. E.; Callow, J. A.; Handlin, D. L.; Willis, C. L.; Kramer, E. J.; Ober, C. K. *Langmuir* **2009**, *25*, 12266–12274.
(13) Evans, L. V. *Bot. Mar.* **1981**, *24*, 167.
(14) Schultz, M. P.; Bendick, J. A.; Holm, E. R.; Hertel, W. M. *Biofouling* **2011**, *27*, 87–98.
(15) Schultz, M. P. *Biofouling* **2007**, *23*, 331–341.
(16) Callow, J. A.; Crawford, S. A.; Higgins, M. J.; Mulvaney, P.; Wetherbee, R. *Planta* **2000**, *211*, 641–647.
(17) Smith, A. M.; Callow, J. A. *Biological Adhesives*; Springer-Verlag: Berlin, Heidelberg, 2006.
(18) Callow, M. E. *Biodeterior. Abstr.* **1996**, *10*, 411–421.
(19) Molino, P. J.; Wetherbee, R. *Biofouling* **2008**, *24*, 365379.
(20) Molino, P. J.; Campbell, E.; Wetherbee, R. *Biofouling* **2009**, *25*, 685–694.
(21) Casse, F.; Stafslien, S. J.; Bahr, J. A.; Daniels, J.; Finlay, J. A.; Callow, J. A.; Callow, M. E. *Biofouling* **2007**, *23*, 121–130.
(22) Kavanagh, C. J.; Quinn, R. D.; Swain, G. W. *J. Adhes.* **2005**, *81*, 843–851.
(23) Tribou, M.; Swain, G. *Biofouling* **2010**, *26*, 47–56.
(24) Omae, I. *Appl. Organometal. Chem.* **2003**, *17*, 81–105.
(25) Yebra, D. M.; Kiil, S.; Dam-Johansen, K. *Prog. Org. Coat.* **2004**, *50*, 75–104.
(26) Sonak, S.; Pangam, P.; Giriyan, A.; Hawaldar, K. *J. Environ. Manage.* **2009**, *90*, S96–108.
(27) Thomas, K. V.; Brooks, S. *Biofouling* **2010**, *26*, 73–88.
(28) Schiff, K.; Diehl, D.; Valkirs, A. *Mar. Pollut. Bull.* **2004**, *48*, 371–377.
(29) Finnie, A.; Williams, D. N. Paint and Coatings Technology for the Control of Marine Fouling. In *Biofouling*; Durr, S., Thomason, J. C., Eds.; Wiley-Blackwell: Chichester, 2010.
(30) Schilp, S.; Rosenhahn, A.; Pettitt, M. E.; Bowen, J.; Callow, M. E.; Callow, J. A; Grunze, M. *Langmuir* **2009**, *25*, 10077–10082.
(31) Bowen, J.; Pettitt, M. E.; Kendall, K.; Leggett, G. J.; Preece, J. A.; Callow, M. E.; Callow, J. A. *J. R. Soc. Interface* **2007**, *4*, 473–477.
(32) Zhang, Z.; Finlay, J. A.; Wang, L.; Gao, Y.; Callow, J. A.; Callow, M. E.; Jiang, S. *Langmuir* **2009**, *25*, 13516–13521.
(33) Aldred, N.; Li, G.; Gao, Y.; Clare, A. S.; Jiang, S. *Biofouling* **2010**, *26*, 673–683.
(34) Andruzzi, L.; Senaratne, W.; Hexemer, A.; Sheets, E. D.; Ilic, B.; Kramer, E. J.; Baird, B.; Ober, C. K. *Langmuir* **2005**, *21*, 2495–2504.
(35) Gudipati, C. S.; Greenlief, C. M.; Johnson, J. A.; Prayongpan, P.; Wooley, K. L. *J. Polym. Sci., Part A: Polym. Chem.* **2004**, *42*, 6193–6208.
(36) Hu, Z.; Finlay, J. A.; Chen, L.; Betts, D. E.; Hillmyer, M. A.; Callow, M. E.; Callow, J. A.; DeSimone, J. M. *Macromolecules* **2009**, *42*, 6999–7007.
(37) Grozea, C. M.; Gunari, N.; Finlay, J. A; Grozea, D.; Callow, M. E.; Callow, J. A; Lu, Z.-H.; Walker, G. C. *Biomacromolecules* **2009**, *10*, 1004–1012.
(38) Schumacher, J. F.; Long, C. J.; Callow, M. E.; Finlay, J. A.; Callow, J. A; Brennan, A. B. *Langmuir* **2008**, *24*, 4931–4937.
(39) Park, D.; Weinman, C. J.; Finlay, J. A.; Fletcher, B. R.; Paik, M. Y.; Sundaram, H. S.; Dimitriou, M. D.; Sohn, K. E.; Callow, M. E.; Callow, J. A.; Handlin, D. L.; Willis, C. L.; Fischer, D. A.; Kramer, E. J.; Ober, C. K. *Langmuir* **2010**, *26*, 9772–9781.
(40) Hopken, J.; Möller, M.; Boileau, S. *New Polym. Mater.* **1991**, *2*, 339–356. Youngblood, J. P.; Andruzzi, L.; Ober, C. K.; Hexemer, A.; Kramer, E. J.; Callow, J. A.; Finlay, J. A.; Callow, M. E. *Biofouling* **2003**, *19*, 91–98.
(41) Xiang, M.; Li, X.; Ober, C. K.; Char, K.; Genzer, J.; Sivaniah, E.; Kramer, E. J.; Fischer, D. A. *Macromolecules* **2000**, *33*, 6106–6119.
(42) Genzer, J.; Sivaniah, E.; Kramer, E. J.; Wang, J. G.; Korner, H.; Xiang, M. L.; Char, K.; Ober, C. K.; DeKoven, B. M.; Bubeck, R. A.; Chaudhury, M. K.; Sambasivan, S.; Fischer, D. A. *Macromolecules* **2000**, *33*, 1882–1887.
(43) Genzer, J.; Kramer, E. J.; Fischer, D. A. *J. Appl. Phys.* **2002**, *92*, 7070–7079.
(44) Sohn, K. E.; Dimitriou, M. D.; Genzer, J.; Fischer, D. A.; Hawker, C. J.; Kramer, E. J. *Langmuir* **2009**, *25*, 6341–6348.
(45) Krishnan, S.; Paik, M.; Ober, C. K.; Martinelli, E.; Galli, G.; Sohn, K. E.; Kramer, E. J.; Fischer, D. A. *Macromolecules* **2010**, *43*, 4733–4743.
(46) Krishnan, S.; Ward, R. J.; Hexemer, A.; Sohn, K. E.; Lee, K. L.; Angert, E. R.; Fischer, D. A.; Kramer, E. J.; Ober, C. K. *Langmuir* **2006**, *22*, 11255–11266.
(47) Schumacher, J. F.; Carman, M. L.; Estes, T. G.; Feinberg, A. W.; Wilson, L. H.; Callow, M. E.; Callow, J. A.; Finlay, J. A.; Brennan, A. B. *Biofouling* **2007**, *23*, 55–62.
(48) Callow, M. E.; Callow, J. A.; Pickett-Heaps, J. D.; Wetherbee, R. *J. Phycol.* **1997**, *33*, 938–947.
(49) Finlay, J. A.; Fletcher, B. R.; Callow, M. E.; Callow, J. A. *Biofouling* **2008**, *24*, 219–225.
(50) Schultz, M. P.; Finlay, J. A.; Callow, M. E.; Callow, J. A. *Biofouling* **2000**, *15*, 243–251.
(51) Andruzzi, L.; Chiellini, E.; Galli, G.; Li, X.; Kang, S. H.; Ober, C. K. *J. Mat. Chem.* **2002**, *12*, 1684–1692.
(52) Mielczarski, J. A.; Mielczarski, E.; Galli, G.; Morelli, A.; Martinelli, E.; Chiellini, E. *Langmuir* **2010**, *26*, 2871–2876.
(53) Finlay, J. A.; Bennett, S. M.; Brewer, L. H.; Sokolova, A.; Clay, G.; Gunari, N.; Meyer, A. E.; Walker, G. C.; Wendt, D. E.; Callow, M. E.; Callow, J. A.; Detty, M. R. *Biofouling* **2010**, *26*, 657–666.